

Fundamental Issues in the Synthesis of Ferroelectric $\text{Na}_{0.5}\text{K}_{0.5}\text{NbO}_3$ Thin Films by Sol–Gel Processing

Anirban Chowdhury,^{*,†} Jonathan Bould,^{†,‡} Michael G. S. Londesborough,[‡] and Steven J. Milne[†]

[†]Institute for Materials Research, Houldsworth Building, University of Leeds, Leeds, LS2 9JT, U.K., and

[‡]Institute of Inorganic Chemistry, Academy of Science of the Czech Republic, 250 68 Řež, Czech Republic

Received December 9, 2009. Revised Manuscript Received May 27, 2010

In contrast to films fabricated by physical vapor deposition methods, thin films of $\text{Na}_{0.5}\text{K}_{0.5}\text{NbO}_3$ (NKN) made by metal alkoxide sol–gel routes generally fail to exhibit polarization–electric field responses typical of a ferroelectric. This study sets out to investigate the reasons for the problems in producing sol–gel NKN films by examining the thermochemistry of the gel to ceramic conversion. The NKN precursor gels displayed multiple heating DTA crystallization exotherms in the temperature range 480–550 °C, which are attributed to compositional segregation of NKN components. At higher temperatures, 800–850 °C, a heating DTA endotherm and cooling DTA exotherm are indicative of melting and recrystallization of sodium/potassium carbonate secondary phases. Additionally, repeated thermal analyses, after storage of the gel decomposition product under ambient conditions, revealed a tendency for hydration and carbonation on exposure to air. Together, these are critically limiting reasons for the absence of strong ferroelectricity in NKN films produced by standard sol–gel methods.

Introduction

Legislation restricting the use of lead-based materials has resulted in an increase in research efforts into fabricating lead-free piezoelectric ceramics with comparable properties to lead zirconate titanate (PZT). Recent studies have shown encouraging results for bulk ceramics of sodium potassium niobate and related solid solution systems.^{1,2} Consequently, there has been considerable interest in the fabrication of bulk and thin-film forms of compositions based on sodium potassium niobate.

In bulk NKN systems, problems arising from the formation of stable secondary niobate phases during sintering, and from the volatility of the alkali metal oxides at high temperatures have been reported.⁶ The uses of various additive sintering oxides have been examined in order to improve densification.³ A number of studies have also been carried out to improve the electrical properties of NKN ceramics, such as the formation of various NKN solid solutions, for example, NKN–LiNbO_3 ,⁴ NKN–LiTaO_3 ,^{5,6}

NKN–LiSbO_3 ,⁷ and $\text{NKN–Li(Nb,Ta,Sb)O}_3$.² As a consequence, intermediate compounds, e.g., $\text{K}_3\text{Li}_2\text{Nb}_5\text{O}_{15}$, have been found to coexist and to interfere with the ferroelectric properties of NKN.^{8,9} Alternatives to solid state reactions have been reported, for example, single-phase KNbO_3 powders may be prepared by a microwave hydrothermal method.⁸ Additions of excess alkali metal carbonates have been shown to minimize the formation of a tungsten bronze $\text{K}_3\text{Li}_2\text{Nb}_5\text{O}_{15}$ phase in NKN–LiTaO_3 made by solid state reaction.⁶ Others have shown that additions of excess NaNbO_3 are beneficial in reducing secondary phases.⁹ In a recent study on the synthesis of sodium potassium niobate from alkaline carbonates and niobium oxide, the issues involved in obtaining a perovskite NKN single-phase product were discussed; phases with compositions $(\text{K,Na})_2\text{Nb}_4\text{O}_{11}$, $\text{K}_4\text{Nb}_6\text{O}_{17}$, and $\text{Na}_2\text{Nb}_4\text{O}_{11}$ were reported to coexist with perovskite NKN.¹⁰ Similar secondary phases, for example, $\text{K}_4\text{Nb}_6\text{O}_{17}$ and $\text{K}_3\text{Li}_2\text{Nb}_5\text{O}_{15}$, have also been reported in sol–gel systems.¹¹

In addition to studies using conventional mixed oxide routes, thin films of $\text{Na}_{0.5}\text{K}_{0.5}\text{NbO}_3$ (NKN) obtained using a variety of physical vapor deposition routes

*Corresponding author. E-mail: anirban.chowdhury@gmail.com (A.C.); S.J.Milne@leeds.ac.uk (S.J.M.). Fax: +81-22-217-5631/+44-113 343 2384.

(1) Guo, Y.; Kakimoto, K.-i.; Ohsato, H. *Mater. Lett.* **2004**, *59*, 241.
(2) Saito, Y.; Takao, H.; Tani, T.; Nonoyama, T.; Takatori, K.; Homma, T.; Nagaya, T.; Nakamura, M. *Nature* **2004**, *432*, 84.
(3) Zuo, R.; Roedel, J.; Chen, R.; Li, L. *J. Am. Ceram. Soc.* **2006**, *89*, 2010.
(4) Guo, Y.; Kakimoto, K.-i.; Ohsato, H. *Appl. Phys. Lett.* **2004**, *85*, 4121.
(5) Guo, Y.; Kakimoto, K.-i.; Ohsato, H. *Mater. Lett.* **2005**, *59*, 241.
(6) Skidmore, T. A.; Milne, S. J. *J. Mater. Res.* **2007**, *22*, 2265.
(7) Lin, D.; Kwok, K. W.; Lam, K. H.; Chan, H. L. W. *J. Appl. Phys.* **2007**, *101*, 074111.

(8) Paula, A. J.; Parra, R.; Zaghete, M. A.; Varela, J. A. *Mater. Lett.* **2008**, *62*, 2581.
(9) Paula, A. J.; Parra, R.; Zaghete, M. A.; Varela, J. A. *Solid State Commun.* **2009**, *149*, 1587.
(10) Malic, B.; Jenko, D.; Holc, J.; Hrovat, M.; Kosec, M. *J. Am. Ceram. Soc.* **2008**, *91*, 1916.
(11) Tanaka, K.; Kakimoto, K.-i.; Ohsato, H.; Iijima, T. *Ferroelectrics* **2007**, *358*, 175.

have been reported, e.g., pulsed laser deposition¹² and magnetron sputtering, and these have resulted in better electrical properties.¹³

Efforts have also been made to fabricate NKN films via sol–gel routes.^{14–18} Söderlind et al.¹⁴ fabricated NKN thin films using an alkoxide, an oxalate, and a modified Pechini method. Extra unidentified XRD peaks were observed in the XRD patterns of the NKN films made by the alkoxide route. Tanaka et al.¹⁵ have reported oriented NKN films deposited on Si/SiO₂ substrates using an alkoxide solution route. The effects of adding excess sodium and potassium reagents¹⁹ and the effect of the Pt bottom layer²⁰ on the properties of films produced from alkoxy-derived precursor solutions have been discussed. The crystallinity of the NKN thin films was found to strongly depend on the relaxation of compressive stress in the as-deposited Pt bottom electrode layers.²⁰ The authors also concluded that to produce high-quality NKN thin films, thermal stability of the microstructure in the Pt bottom electrode layers was required.

Lai et al.¹⁶ synthesized a starting sol by reacting Na and K metals with ethanol and 2-methoxyethanol: acetic acid and acetylacetone were added as chelating agents prior to the addition of a stoichiometric amount of niobium pentaethoxide [Nb(OC₂H₅)₅]. Nakashima et al.^{17,18} investigated the structural and electrical properties of the resultant NKN films with different amounts of excess sodium and potassium. The leakage current and ferroelectric properties of the perovskite KNN thin films were found to be strongly affected by the excess amounts of K and Na as well as the heating conditions of the precursor films; no saturation was observed in their reported polarization–electric field (P–E) hysteresis loops. Wu et al. made NKN films with sodium and potassium acetates and niobium ethoxide.²¹ Kim et al.²² have also synthesized (Na_xK_{1-x})NbO₃ thin films by the alkoxide-based sol–gel method.

However, in examples of sol–gel synthesis of NKN films, where P–E measurements were carried out, little evidence of ferroelectricity was observed, or only a faint contribution was evident in combination with a strong component from dielectric loss.^{16,17,19,21} This contrasts with the situation for NKN films deposited by physical vapor deposition where a nonlinear hysteretic P–E re-

ponse typical of a ferroelectric has been recorded.^{12,13,23} Hence, the absence of ferroelectric behavior seems to be a specific problem for solution-based processing of NKN films and not to the generic characteristics of NKN films.

The aim of the present work is to investigate the reasons for the absence of ferroelectricity in NKN films prepared from metal alkoxide based sol–gel routes by undertaking a detailed analysis of the chemical changes taking place during the gel to ceramic conversion.

Experimental Section

Sodium and potassium “ingots” and 2-methoxyethanol were purchased from Sigma-Aldrich and niobium ethoxide from Alfa-Aesar. In a nitrogen filled glovebox, and after washing with dry hexane, pieces of the appropriate metal were cut with a scalpel and the outer oxidized edges removed. The remaining fraction was then weighed inside the glovebox. Individual methoxyethoxide sols of Na and K were prepared by magnetically stirring pieces of the metal in 2-methoxyethanol in a round bottomed flask until hydrogen evolution had ceased. The individual methoxyethoxide precursors of sodium and potassium were then mixed with a calculated amount of niobium ethoxide to make a Na_{0.5}K_{0.5}NbO₃ sol of concentration 0.5 M, and the stoppered flask was put on a magnetic stirrer for 90 min. The flask was then removed from the glovebox, attached to a reflux condenser against a flow of nitrogen, and allowed to reflux (125 °C) for 0, 24, and 70 h, respectively. To obtain a dry gel, the NKN stock solution was maintained at 60–70 °C with slow stirring for 4 h and then ground into a fine powder using an agate mortar and pestle.

Thermal analyses of the NKN gels were carried out on the dried sol powders using simultaneous thermogravimetric analysis (TGA) and differential thermal analysis (DTA) [Netzsch STA 409, QMG 420]. The dried gel sample was heated to 950 at 8 °C min⁻¹ in air, and the evolved gases were examined by mass spectrometry. In this work, DTA peak temperatures, as opposed to onset temperatures, are reported.

NKN thin-film samples were made by depositing the 0.5 M sols (nonrefluxed) onto platinized silicon substrates using a spin-coating technique, with a two step hot plate heating process: 250 °C for 5 min and 500 °C for 5 min, followed by furnace heating to 650 °C. Final films were ~0.2 μm in thickness. Phase analysis of the NKN thin films was carried out at room temperature using an X-ray diffractometer (Philips APD 1700, Almelo, The Netherlands) with monochromic Cu–K_α radiation (λ = 1.5418 Å). Fourier transform infrared analysis (FTIR) of the thin films was conducted using a Bruker (Vertex-70) IR spectrophotometer over the wavelength range 4000–400 cm⁻¹. For electrical testing, the P–E responses were examined using a RT66A ferroelectric tester (Radiant Technologies, Albuquerque, NM) at a frequency of 1 kHz.

Results

Nonrefluxed NKN Gel. The TGA, DTG, DTA, and mass spectrometry data for the NKN gel sample without reflux are shown in parts a and b of Figure 1. The main TGA mass loss (~13.5 mass %) occurred at temperatures up to 200 °C (DTG peak 109 °C), with a further incremental loss (~1.4 mass %) between 200 and 327 °C,

- (12) Cho, C.-R.; Grishin, A. *Appl. Phys. Lett.* **1999**, *75*, 268.
- (13) Khartsev, S.; Grishin, A.; Andreasson, J.; Koh, J.-H.; Song, J.-S. *Integr. Ferroelectr.* **2003**, *55*, 769.
- (14) Soederlind, F.; Kaell, P.-O.; Helmersson, U. *J. Cryst. Growth* **2005**, *281*, 468.
- (15) Tanaka, K.; Kakimoto, K.-i.; Ohsato, H. *J. Cryst. Growth* **2006**, *294*, 209.
- (16) Lai, F.; Li, J.-F. *J. Sol-Gel Sci. Technol.* **2007**, *42*, 287.
- (17) Nakashima, Y.; Sakamoto, W.; Maiwa, H.; Shimura, T.; Yogo, T. *Jpn. J. Appl. Phys.* **2007**, *46*, L311.
- (18) Nakashima, Y.; Sakamoto, W.; Shimura, T.; Yogo, T. *Jpn. J. Appl. Phys.* **2007**, *46*, 6971.
- (19) Tanaka, K.; Hayashi, H.; Kakimoto, K.-i.; Ohsato, H.; Iijima, T. *Jpn. J. Appl. Phys.* **2007**, *46*, 6964.
- (20) Tanaka, K.; Kakimoto, K.-i.; Ohsato, H.; Iijima, T. *Jpn. J. Appl. Phys.* **2007**, *46*, 1094.
- (21) Wu, X.; Wang, L.; Ren, W.; Yan, X.; Shi, P.; Chen, X.; Yao, X. *Ferroelectrics* **2008**, *367*, 61.
- (22) Kim, K.-T.; Kim, G.-H.; Woo, J.-C.; Kim, C.-I. *Ferroelectrics* **2007**, *356*, 166.

- (23) Lee, J. S.; Lee, H. J.; Lee, J. Y.; Kang, S. H.; Kim, I. W.; Ahn, C. W.; Chung, G. S. *J. Korean Phys. Soc.* **2008**, *52*, 1109.

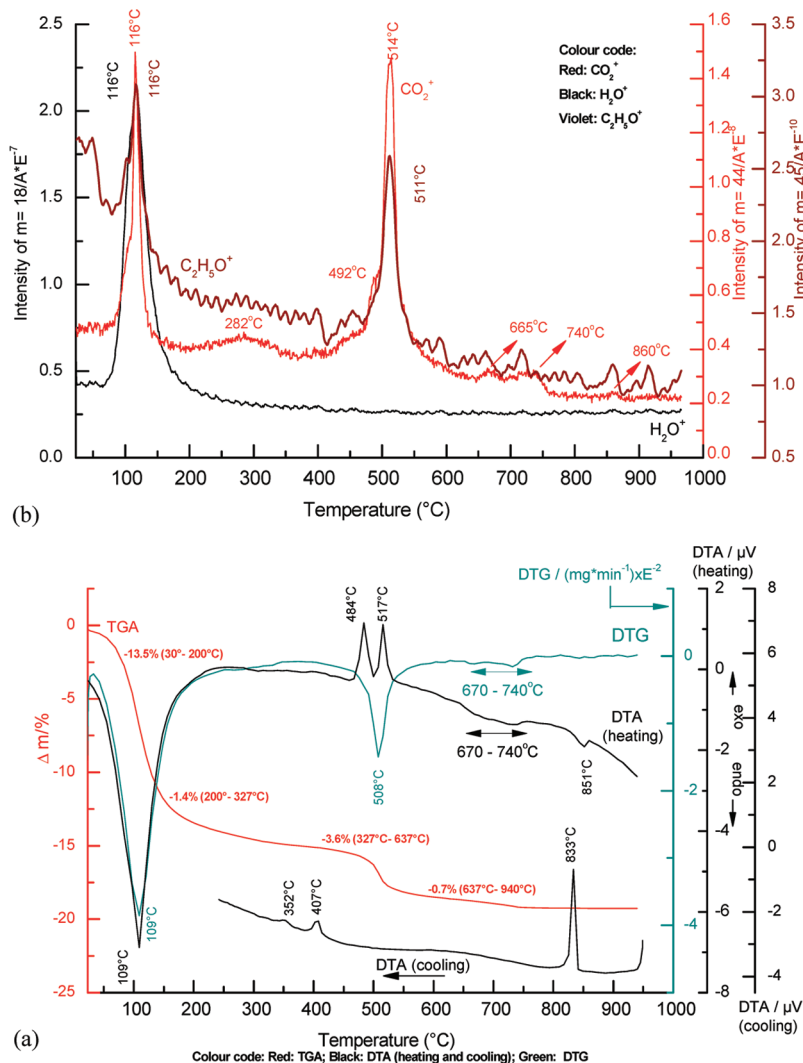


Figure 1. (a) TGA, DTG, DTA, and (b) mass spectrometry of the evolved gases plots for the nonrefluxed NKN gel.

Figure 1a. The DTA heating plot shows a strong endotherm at 109 °C and two exothermic peaks at 484 and 517 °C, Figure 1a. There is also a faint broad DTA endotherm (also observed in the DTG plot) between 670 and 740 °C with an accompanying mass loss of ~ 0.7 mass %. Finally, a weak DTA heating endotherm, with no change in sample mass, occurs at 851 °C. The DTA cooling cycle shows a very strong sharp exotherm at 833 °C that we presume to be associated with the reverse of the latter heating phase change. Other cooling DTA exotherms appeared at 407 and 352 °C with no mass change.

Complementary evolved gas mass spectrometry, Figure 1b, shows that the low-temperature TGA mass loss (≤ 200 °C) corresponds to the elimination of water, ethanol, and carbon dioxide from the gel; no evidence of methoxyethanol vapors was observed. There is also evidence of a minor amount of CO_2 being evolved over the temperature range 250–350 °C; evolution of CO_2 could be the reason for the slight change in the slope of the TGA plot and the slight deviation in the DTG plot in this temperature region, Figure 1a. The CO_2 peaks centered on 492 and 514 °C indicate that the two DTA heating

exotherms at 484 and 517 °C coincide with the decomposition of inorganic carbonate phases. Carbonate decomposition is expected to be endothermic, and therefore, the two exotherms at 484 and 517 °C can be attributed to crystallization events which occur immediately upon decomposition of the carbonate precursors. However, the detection of $[\text{C}_2\text{H}_5\text{O}]^+$ fragments in this temperature range indicates that an organic component is also undergoing thermal decomposition. At higher temperatures, faint intensity CO_2 mass spectrometry peaks at 665 and 740 °C coincide with the faint DTA and DTG anomalies between 670 and 740 °C indicating further carbonate decompositions are taking place. The final faint DTA peak on heating at 851 °C also appears to show a very faint CO_2 evolution at 860 °C, but this is indistinct.

The cooling DTA cycle reveals an exothermic sharp peak at 833 °C which is considered to be the analogue of the 851 °C heating peak. The intensity and sharp profile of this peak suggests it may be linked to a crystallization event on cooling; its origins are discussed later in the text.

Further information on the thermochemistry was obtained by subjecting the sample after the first heat-cool

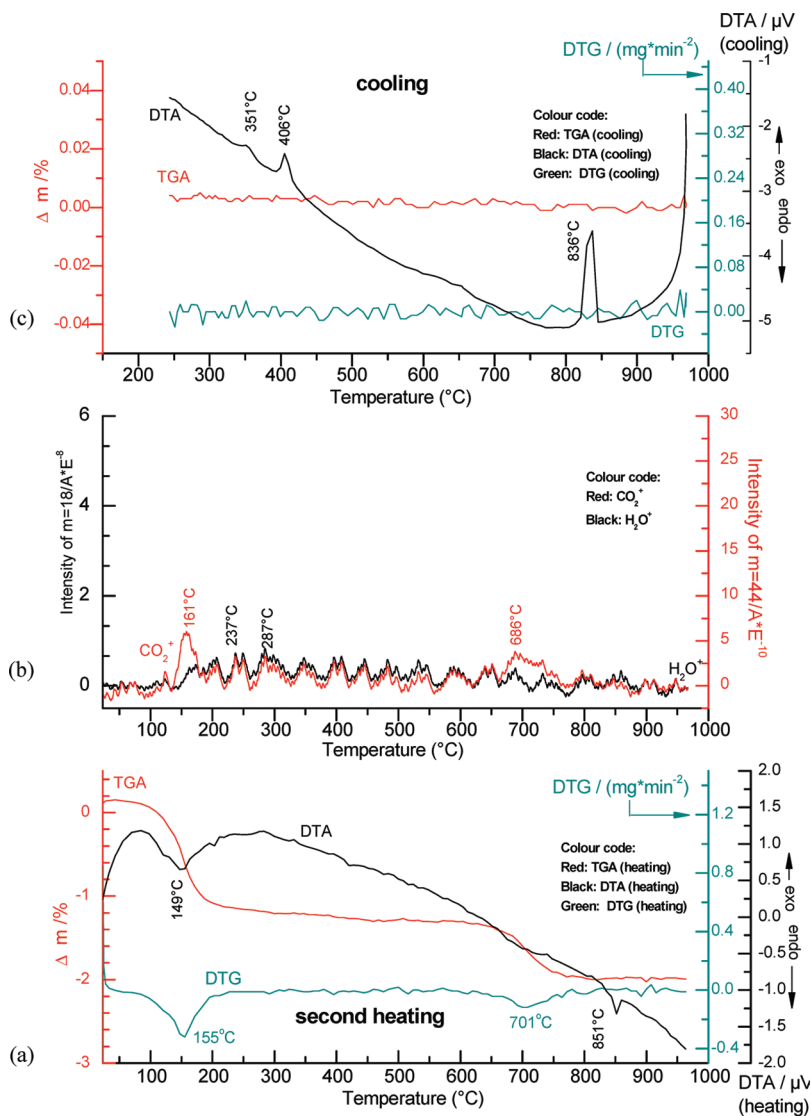


Figure 2. (a) and (c) TGA, DTG, and (b) mass spectrometry of the evolved gases plots for the nonrefluxed NKN gel carried out during a second heat–cool cycle after 80 days.

cycle to a second heat–cool cycle after being stored in air for 80 days. Similarly to that for the first heat–cool cycle, the second TGA plot, Figure 2a, also shows a loss of mass at low temperature, but of only 1.1 wt %, which levels off at 180 °C and is accompanied by a corresponding DTA endotherm. These observations indicate that the NKN powder reacted with atmospheric CO_2 during storage. This may involve the formation of a bicarbonate or a weakly bound carbonate species formed by adsorption of CO_2 from the atmosphere; various types of these adsorbed carbonates have already been reported.^{24,18}

There is also a 0.7 mass % loss with CO_2 evolution at 670–740 °C, similar to the first run, indicating another more stable carbonate was also formed on exposure to air, Figure 2b. The DTA peak at 851 °C seen in the first run is also present, as is the cooling DTA peak at 836 °C, Figure 2c.

NKN Gel (Refluxed for 24 h). Heating the sols under reflux conditions for 24 h prior to gelation produced a

number of noteworthy differences in thermal evolution as shown in Figure 3a. A broad DTA exotherm peak (weak–medium) occurred in the temperature range 330–490 °C with corresponding mass losses evident in the non-refluxed sample. There was also a change in the temperature of the sharp midrange exotherms which now occurred at 510 and 537 °C as opposed to 484 and 517 °C for the non-refluxed sample. Moreover, the relative intensity of the two peaks differed, with the higher temperature, 537 °C, peak now being of greater intensity. This suggests differences in the composition and proportions of the crystallizing phases. Other features were similar to those of the non-refluxed sample, although the intensities of the high temperature peak at 850 °C and cooling exotherm at 833 °C were lower than for the non-refluxed sample.

In contrast to the nonrefluxed sample, fragments consistent with methoxyethanol were detected (mass number = 76) around 100 °C. The broad, multiple DTA peaks at midtemperatures, ~330–550 °C gave rise to

(24) Davydov, A. *Molecular Spectroscopy of Oxide Catalyst Surfaces*; John Wiley & Sons: Chichester, U.K., 2003; pp 133–139.

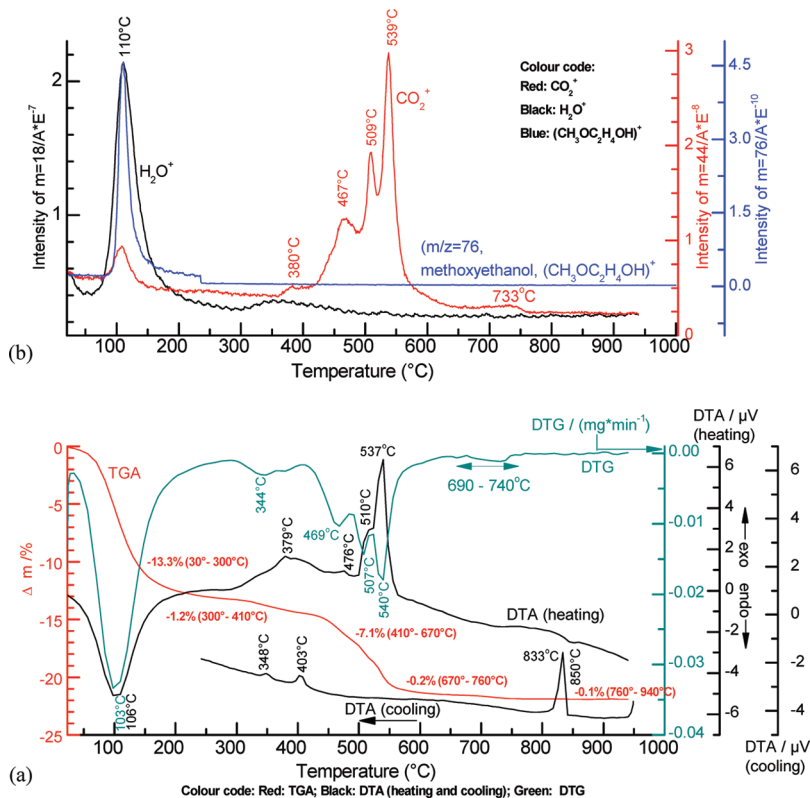


Figure 3. (a) TGA, DTG, DTA, and (b) mass spectrometry of the evolved gases plots for the 24 h refluxed NKN gel.

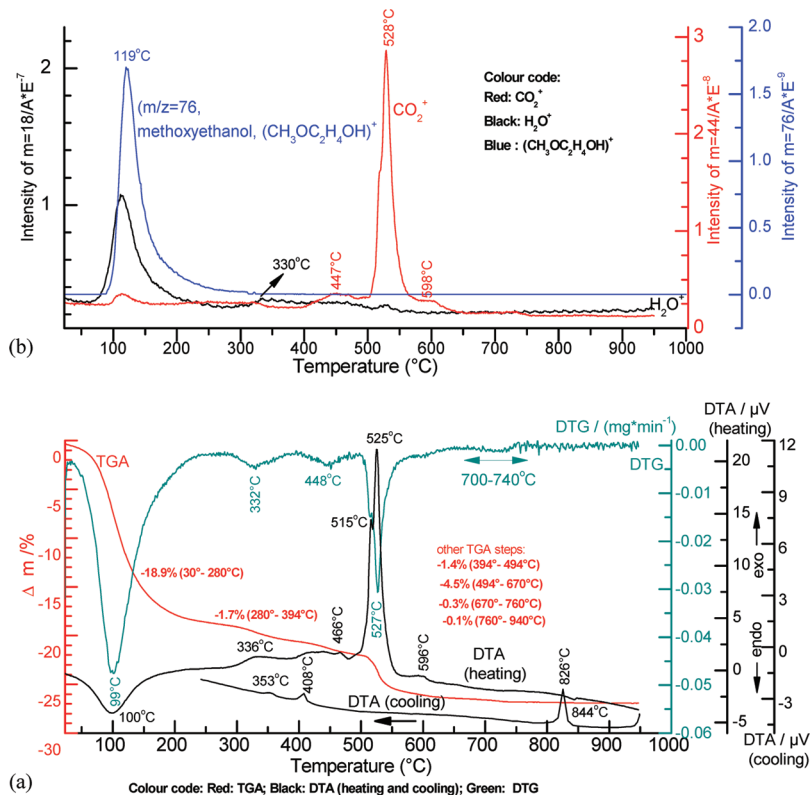


Figure 4. (a) TGA, DTG, DTA, and (b) mass spectrometry of the evolved gases plots for the 70 h refluxed NKN gel.

corresponding CO_2 evolution peaks indicating carbonate phases were present over this temperature range. A small peak for CO_2 can be noticed at 733 °C, with a corresponding DTG broad peak around 690–740 °C, but here

the carbonate peak intensity is smaller than in the case of the nonrefluxed sample, Figure 3b.

NKN Gel (Refluxed for 70 h). Refluxing for 70 h produced further changes, Figure 4. The weak DTA

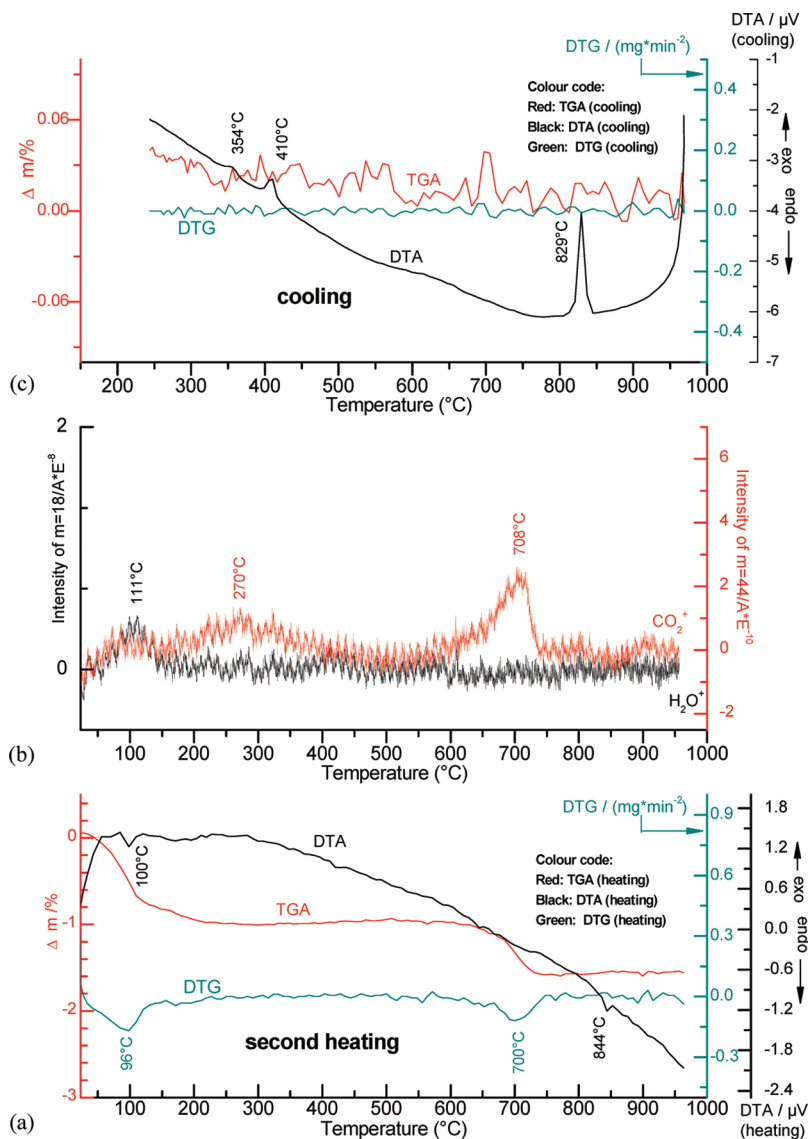


Figure 5. (a) and (c) TGA, DTG, DTA, and (b) mass spectrometry of the evolved gases plots for 70 h refluxed NKN gel carried out during a second heat–cool cycle after 80 days.

heating exotherms in the midtemperature range, 330–550 °C were again present but occurred at slightly different temperatures compared to the 24 h sample. The two strongest DTA exotherms showed a further shift in temperature, with peak temperatures of 515 and 525 °C, as opposed to 510 and 537 °C for the 24 h refluxed NKN gel. Hence the peak temperatures converge as the refluxing time increases although two distinct peaks are still distinguishable even after 70 h reflux time. A small DTA peak at 596 °C is a new feature, Figure 4a. The high temperature DTA heating endotherm and cooling exotherm at 844 and 826 °C, respectively, continued to be present but were of further reduced intensity compared to the 24 h sample. The cooling weak DTA endotherms occurred at comparable temperatures, 408 and 353 °C, to the previous samples. The origin of these and discussed in the next section.

Evolved gas analysis for the 70 h sample showed an increased intensity of the methoxyethanol mass spectrometry peak at 119 °C relative to 24 h reflux, Figure 4b. The CO₂ peak was decreased but the fragment linked to

methoxyethanol evaporation (at 119 °C) was now stronger. The midtemperature decomposition of inorganic carbonates was confirmed by CO₂ evolution. A weak H₂O peak around ~330 °C corresponds to the DTA peak at 336 °C indicating decomposition of a hydrated phase with a hydrated carbonate being possible as small amounts of CO₂ were also evolved. The DTA exotherm at 596 °C is linked to CO₂ evolution, indicating another carbonate decomposition product is produced for the longer reflux time.

A second heat–cool cycle, after 80 days storage in a screw cap sample tube, showed a TGA step at ~100 °C linked to H₂O and CO₂ evolution and ~710 °C linked to CO₂ evolution, Figures 5a–c, similar to the second heat–cool cycle for the 24 h reflux time.

The three NKN gels showed an increased in total mass % loss as the reflux time increased from 0 h (19.2%) to 24 h (21.9%) and finally to 70 h (26.9%). The main steps in the decomposition of the three samples are summarized in Table 1.

Table 1. Keynote Points Obtained from the Thermal Analysis of the NKN Dried Gels

plots	NKN sol made with different refluxing time		
	nonrefluxed	refluxed 24 h	refluxed 70 h
TGA	i. major ~13 mass % loss up to 170 °C; total mass loss ~19% until 950 °C ii. 2nd heat-cool cycle shows a mass loss (~1%) around 120–250 °C and between 670 and 760 °C (~0.7%)	similar pattern as nonrefluxed sol, total mass loss ~22% until 950 °C	i. major ~17 mass % loss up to 170 °C; total mass loss ~27% until 950 °C ii. 2nd heat-cool cycle shows a mass loss (~0.6%) around 70–170 °C and between 660 and 720 °C (~0.5%)
DTG	i. peaks at 109 °C (sharp), 508 °C (sharp), and 740 °C (small) ii. 2nd heat-cool cycle shows peaks at 155 °C and around 700 °C	peak at 109 °C (sharp), multiple peaks around 330–550 and 733 °C (small)	i. peaks at 100 °C (sharp), 332 °C (weak), 527 °C (sharp), and 726 °C (weak) ii. 2nd heat-cool cycle shows peaks at 96 °C and around 720 °C
DTA (heating)	i. peaks at 109 °C (endo), 484 °C (exo), 517 °C (exo), 740 °C (broad), and 851 °C (endo) ii. 2nd heat-cool cycle shows peaks at 149 °C (endo) and 851 °C (endo)	i. multiple weak exo peaks around 330–500 °C ii. strong peaks at 510 °C (exo) and 537 °C (exo) and weak peak at 850 °C (endo)	i. peaks at 100 °C (endo), 336 °C (exo), 466 °C (exo), 515 °C (shoulder, exo), 525 °C (sharp, exo), 596 (weak, exo), and 844 °C (weak, endo) ii. 2nd heat-cool cycle shows peaks at 100 °C (endo) and 844 °C (endo)
DTA (cooling)	i. very sharp peak at 851 °C (exo) and 407 °C (exo), 351 °C (exo) ii. 2nd heat-cool cycle shows peaks at 836 °C (exo), 406 °C (exo), and 351 °C (exo)	sharp peak at 851 °C (exo) and 403 °C (exo), 348 °C (exo)	i. peak at 826 °C (exo) and 408 °C (exo), 353 °C (exo) ii. 2nd heat-cool cycle shows peaks at 829 °C (exo), 410 °C (exo) and 354 °C (exo)
mass spectrometry	C ₂ H ₅ O ⁺ fragments at 116 °C, 511 °C, H ₂ O ⁺ fragments at 116 °C, CO ₂ ⁺ fragments at 116 °C (strong), 284 °C (broad), 487 °C (shoulder), 517 °C (strong)	i. evidence for water, ethanol, methanol, 2-methoxyethanol, and CO ₂ evolution around ~100 °C ii. peaks for CO ₂ at 380 °C, 467 °C, 509 °C, 539 °C, and 733 °C (weak)	i. peaks for water, ethanol, methanol, 2-methoxyethanol, and CO ₂ evolution around ~110 °C ii. peaks for CO ₂ at 447 °C, 518 °C, 528 °C, 598 °C (weak) iii. 2nd heat-cool cycle show peaks for CO ₂ at 270 °C and 708 °C; peak for water at 110 °C

Discussion

For the series of NKN gels (0, 24, and 70 h refluxed), a notable feature of the lower-temperature plots was the gradual intensification of the mass spectrometry peak for a methoxyethanol fragment around 110–120 °C as the refluxing times were increased. Considering that the Na and K metal precursors were dissolved in methoxyethanol to form methoxide starting reagents, this finding is consistent with reflux operations promoting condensation reactions between the components to form oligomeric species, liberating methoxide ligands. Any ethanol would have evaporated during the drying stage (60 °C for 4 h) prior to thermal analysis. Improved chemical homogeneity at the molecular level is anticipated from the longer reflux times.

Refluxing led to a series of carbonate intermediate phases which decompose over the temperature range, 350–500 °C. These carbonates form by reaction between the residue and evolved (methoxyethanol) vapors. The phases responsible for CO₂ evolution at lower temperatures, ~110 °C, are probably bicarbonates of Na and K which typically undergo low-temperature decomposition.²⁵

For all three NKN gels, an important feature is the presence of exothermic DTA peaks in the range 480–

540 °C (484 and 517 °C for nonrefluxed, 510 and 537 °C for 24 h refluxed, and 515 and 525 °C for the 70 h refluxed NKN gels, respectively). These appear to be crystallization peaks, but the coincident evolution of CO₂ indicates that the crystallization is a consequence of a carbonate precursor phase which crystallizes immediately upon the carbonate being converted to an oxide. The exothermic crystallizations dominate over the associated (endothermic) carbonate decomposition reactions. On the basis of this interpretation, two crystallization peaks are signified in each of the NKN gels. This suggests that crystalline, single phase NKN is not formed directly from the gel decomposition product (metal oxides/carbonates), signifying phase segregation in the gels/decomposing gels. These could be Na-rich and K-rich NKN solid solutions as opposed to the desired Na_{0.5}K_{0.5}NbO₃ phase. Although the changes in peak temperatures indicate a convergence in composition as reflux times increase, even after 70 h of prolonged refluxing, a single crystallization peak for the NKN gels could not be obtained. To help elucidate these and other features, the thermal decomposition of NaNbO₃ and KNbO₃ gels (refluxed 70 h) prepared from the same precursors were examined, Figures 6 and 7. The single crystallization peak in each case (for the 70 h refluxed case) occurs at 612 and 683 °C, respectively, indicating that the two component crystallizations in the NKN gels are not simply the binary K or Na niobates. They are probably two NKN compositions

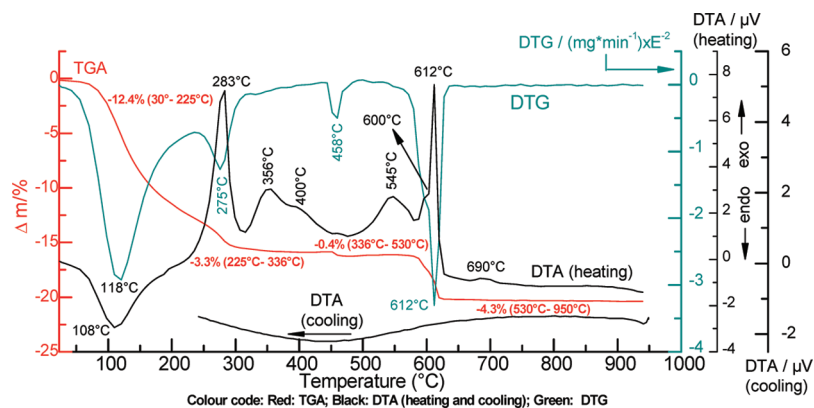


Figure 6. TGA, DTG, and DTA plots of the evolved gases plots for the NaNbO_3 precursor gel refluxed for 70 h.

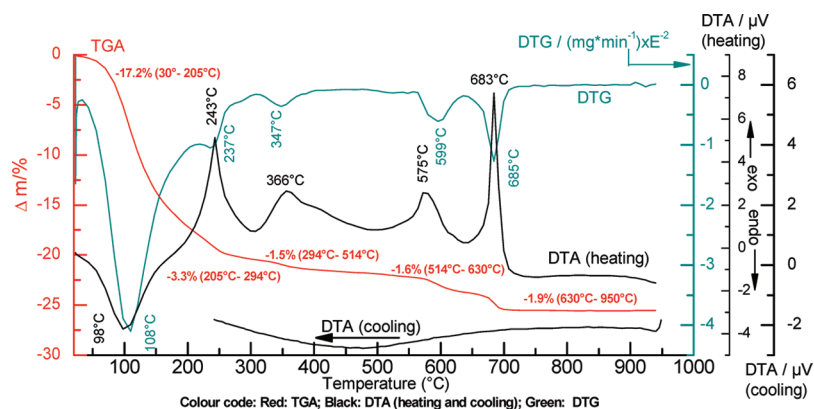


Figure 7. TGA, DTG, and DTA plots of the evolved gases plots for the KNbO_3 precursor gel refluxed for 70 h.

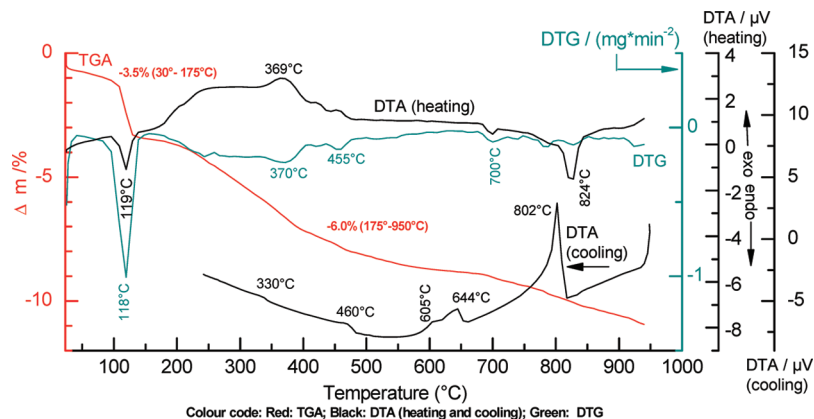


Figure 8. TGA, DTG, and DTA plots of the evolved gases plots for the nonrefluxed Na methoxyethoxide gel.

each differing from the desired $\text{Na}_{0.5}\text{K}_{0.5}\text{NbO}_3$ phase. As reflux time increases, the compositions of these phases more closely approach the 50/50 ratio, but even a 70 h reflux time is insufficient to produce a $\text{Na}_{0.5}\text{K}_{0.5}\text{NbO}_3$ single phase product. This suggests that refluxing the Na and K methoxides prior to introducing the Nb reagent could be beneficial and should be studied in future work. However, the result also implies that the reaction between Nb ethoxide and the alkali metal reagents could be quite slow and so a more fundamental chemical investigation of these reactions could be informative.

The endothermic peak in the DTA heating cycle around 825–850 °C probably denotes a phase change and

possible phase melting. In the case of a K methoxyethoxide gel, there is a DTA peak at 881 °C whereas a peak occurs at 824 °C for Na methoxyethoxide gel decomposition (see Figures 8 and 9). These are close to the melting temperatures of the respective carbonates. Reference to the literature²⁶ indicates that K_2CO_3 melts at 901 °C and Na_2CO_3 at 854 °C. Hence, in NKN gels, the corresponding peak at the slightly lower temperatures 825–850 °C is probably indicative of a small amount of secondary carbonate phase melting and, on cooling, crystallizing to give a sharp cooling exotherm. The phase diagram for

(26) Reisman, A. *J. Am. Chem. Soc.* **1959**, *81*, 807.

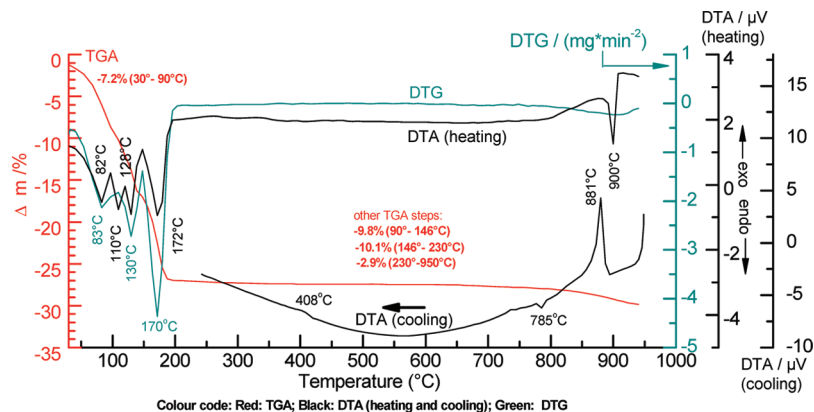


Figure 9. TGA, DTG, and DTA plots of the evolved gases plots for the nonrefluxed K methoxyethoxide gel.

$\text{K}_2\text{CO}_3\text{--Na}_2\text{CO}_3$ indicates a minimum melting temperature for a binary mixture at 710 °C, and so the ~ 850 °C temperature range of the heating peak in the NKN system suggests there could be some degree of mixing of Na and K carbonates.²⁶

The cooling DTA exotherms showed a faint exotherm at around 400–410 °C. In the $\text{NaNbO}_3\text{--KNbO}_3$ system, a phase change between tetragonal and cubic phases occurs in this temperature range for NKN solid solutions, although the 50/50 composition has a slightly higher transition temperature, just over 400 °C.^{27,28}

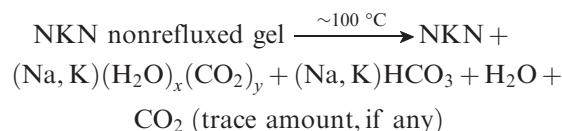
A second cooling DTA exotherm occurs at around 350 °C. This does not coincide with any transition in the $\text{NaNbO}_3\text{--KNbO}_3$ phase diagram, but there is a transition at 350–360 °C for NaNbO_3 and solid solutions containing up to ~ 2 mol % KNbO_3 .²⁹ However, there is also a report of a phase transition at 354 °C for a (50–50) $\text{Na}_2\text{CO}_3\text{--Nb}_2\text{O}_5$ composition.²⁶ If the peak were due to sodium carbonate, it would complement the supposition that the > 800 °C peak is from Na_2CO_3 . Indeed, DTA studies on Na_2CO_3 indicate reversible phase transformations of Na_2CO_3 at 359 and 485 °C, respectively.³⁰ However, we observed no peak at 485 °C, and thus we are not able to reach any firm conclusion on this point. A Na_2CO_3 or K substituted Na_2CO_3 secondary phase would nevertheless be consistent with compositional deviations in the main product and the failure to identify a single $\text{Na}_{0.5}\text{K}_{0.5}\text{NbO}_3$ crystallization event in the midtemperature range. The presence of two NKN phases each differing in composition from $\text{Na}_{0.5}\text{K}_{0.5}\text{NbO}_3$ would contribute to poor electrical properties as would the presence of the secondary carbonate phases.

A summary of the main features of these three NKN systems is given in Table 1, and a brief interpretation of the process chemistry of these thermal events is shown in Figure 10.

The CO_2 peaks on the second heating are indicative of inorganic carbonate phases formed due to exposure to

atmospheric CO_2 on standing. For the nonrefluxed gel, there are at least two types of carbonate in the second run, viz those decomposed at < 180 °C and those at 650–740 °C. The presence of an H_2O peak at 111 °C and CO_2 mass spectrometry peaks at 111 and 708 °C (Figure 2b) in the 70 h refluxed NKN gel indicate that the former may be a bicarbonate or a weakly bound carbonate formed by adsorption of CO_2 from the atmosphere; various types of these adsorbed carbonates have been reported.²⁴ It has been noted that both hydrated sodium and potassium carbonates have sharp phase transitions indicating water loss from the system around this temperature region (70–180 °C).³¹ The higher temperature exotherm on the second run indicates a stable metal carbonate is also formed on reaction with air. This is in addition to the persistence of the Na/KCO_3 phase.

The overall decomposition for this second heating for this temperature range may be tentatively shown as



This is an important result indicating the sensitivity of the NKN powders to reaction with atmospheric CO_2 . It is probable that the bicarbonate or carbonate, which is only stable below ~ 170 °C, is a consequence of room-temperature exposure to air.

Because of the presence of Na/KCO_3 (or related secondary carbonate phase) and the propensity for reaction with atmospheric CO_2 , giving rise to inhomogeneous NKN products, then films made from this sol–gel route are unlikely to display ferroelectric properties. This was indeed found to be the case, Figure 11. It may well be that reaction between the secondary Na/KCO_3 phase and air exacerbates problems of reactivity (formation of related carbonates), making sol–gel derived NKN films more susceptible to carbonate contamination than NKN films produced by physical vapor deposition. It could also be possible that, for the two alkali metal alkoxides, the affinity between K and Na methoxyethoxides inhibits

(27) Shirane, G.; Newnham, R.; Pepinsky, R. *Phys. Rev.* **1954**, *96*, 581.

(28) Tennery, V. J.; Hang, K. W. *J. Appl. Phys.* **1968**, *39*, 4749.

(29) Mishra, S. K.; Choudhury, N.; Chaplot, S. L.; Krishna, P. S. R.; Mittal, R. *Phys. Rev. B* **2007**, *76*, 024110.

(30) Cook, L. P.; McMurdie, H. F.; Ondik, H. M. *Phase Diagrams for Ceramists*, Vol. 7; American Ceramic Society: Westerville, OH, 1989.

(31) Liptay, G. *Atlas of Thermoanalytical Curves*; Heyden & Son: London, 1973.

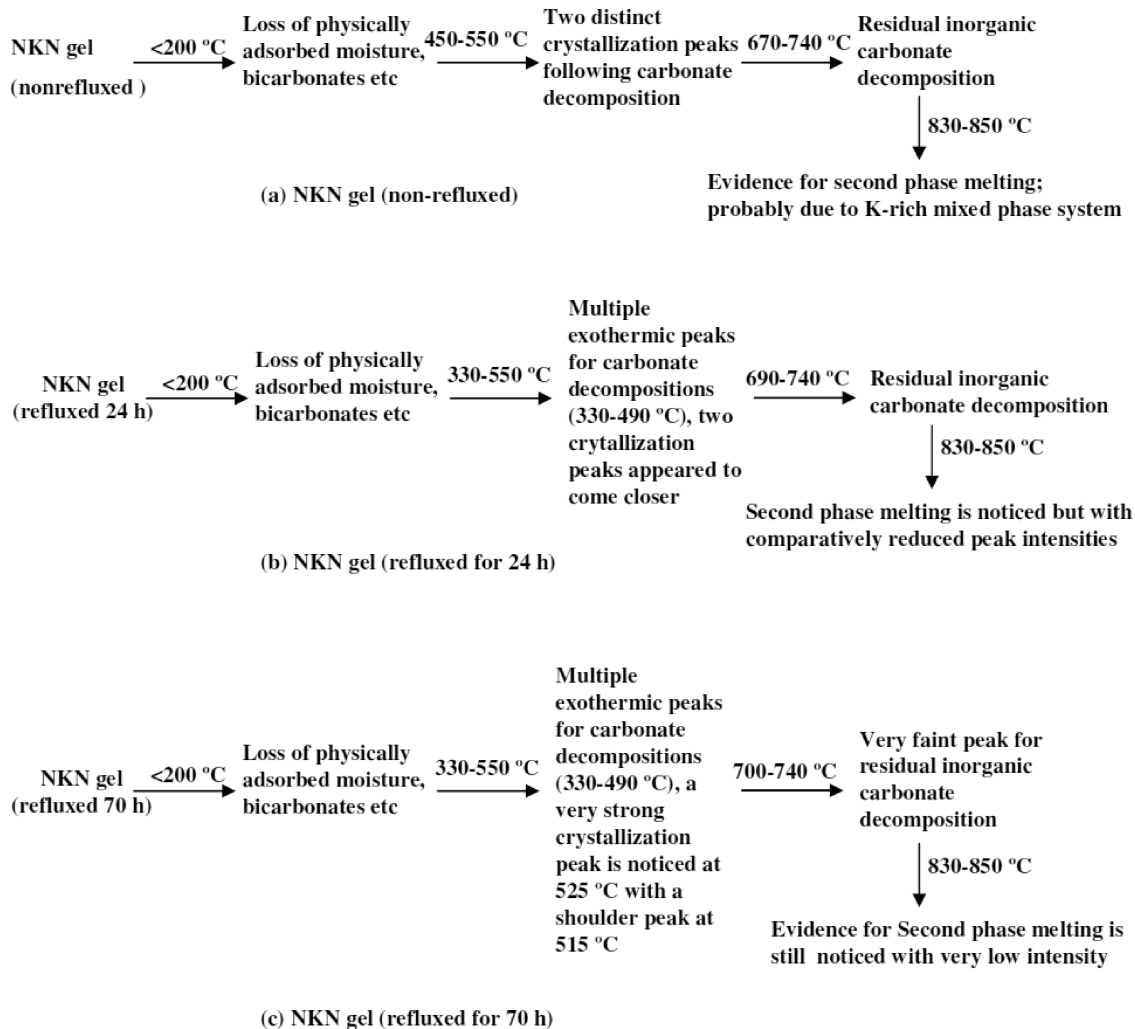


Figure 10. Summarized flow diagrams for the key thermochemical events occurring in the different NKN gels.

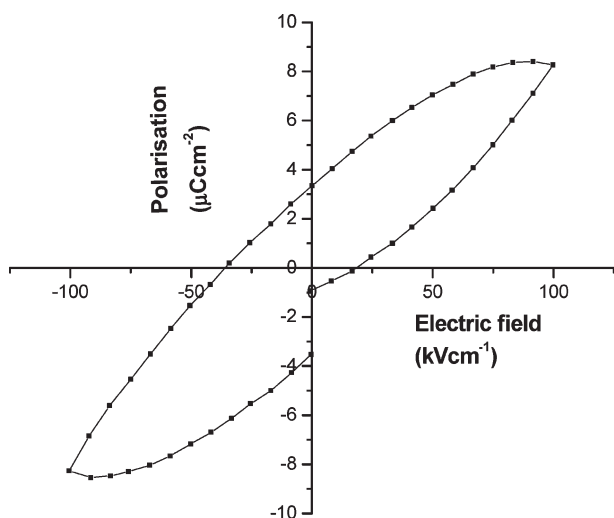


Figure 11. A representative polarization-electric field loop for films made with NKN sol refluxed for 70 h.

reaction with Nb ethoxide, which probably promotes some Na/K carbonate formation. Therefore, extreme care was taken in the cleaning and weighing out of the Na and K metal in order to minimize the possibility of compositional deviations arising from this step.

X-ray diffraction patterns of NKN thin films made from these sols showed additional peaks, notably at $10.5^\circ 2\theta$, as seen in the film made from a nonrefluxed sol, and at $44.5^\circ 2\theta$ in the case of a 70 h refluxed NKN sol, indicating that a secondary crystalline phase was present, Figure 12. However, comparisons with reference XRD files failed to unambiguously identify these phases (as carbonates or inorganic compounds reported in bulk ceramic NKN samples), although the results of thermal analysis suggest that some form of hydrated carbonate phase is present. The NKN peaks in Figure 12 are indexed on the basis of a pseudocubic unit cell. The peak splitting characteristic of orthorhombic NKN⁶ was not observed, presumably due to broadening effects associated with fine crystallite size and the chemical inhomogeneity in NKN composition inferred from thermal analysis.

The formation of one or more intermediate surface carbonate(s) in thin film samples is confirmed by FTIR analysis of an NKN thin film (made from a nonrefluxed sol) which had been heated at $650\text{ }^\circ\text{C}$, Figure 13. Peaks at 1425 cm^{-1} (CO_3^{2-} bending) and 1350 cm^{-1} (COO^- stretching) signify the presence of noncoordinated and bidentate carbonates.³²

(32) Gensse, C.; Anderson, T. F.; Fripiat, J. J. *J. Phys. Chem.* **1980**, *84*, 3562.

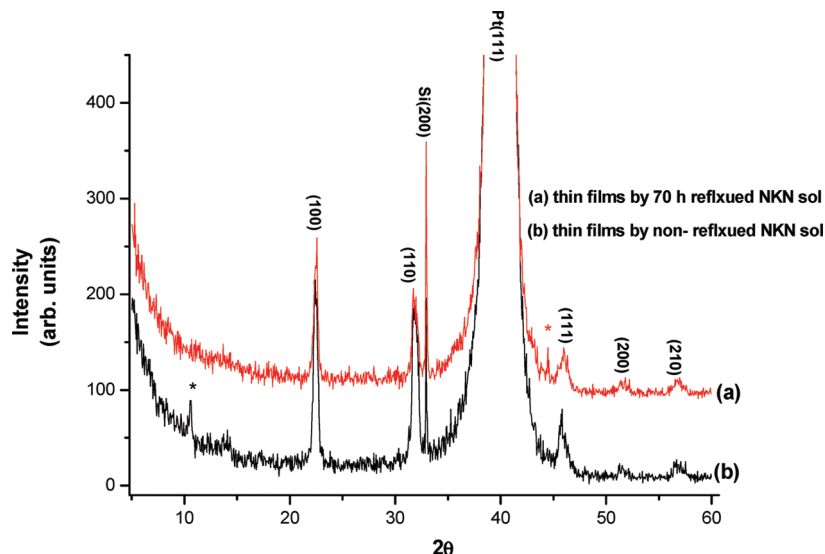


Figure 12. X-ray diffraction pattern of films made from NKN sols heated at 700 °C (30 min). * indicates main extra peak.

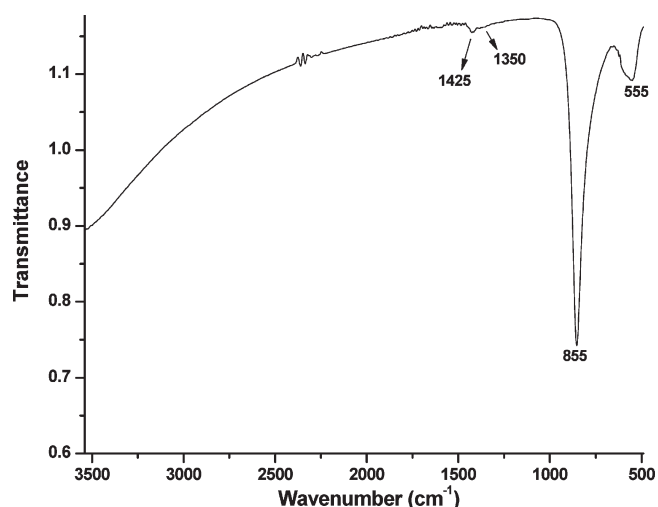


Figure 13. FTIR plot of a NKN thin film made from a nonrefluxed sol heated at 650 °C.

The foregoing results indicate that the carbonate phase(s) persist to temperatures above the thermal limit of the commonly used Si substrates (700–750 °C). Even if reaction with air could be avoided, the residual carbonate phase (indicated by the 850 °C DTA peak) arising from compositional segregation is a significant feature in these sol–gel derived samples.

Good-quality ferroelectric NKN films may be made by MOCVD using precursors such as tetramethylheptandionates, involving a different chemical process to sol–gel, in which the decomposition reaction takes place at the vapor/solid interface in flowing oxygen at temperatures of ~700 °C.³³ These vapor-phase molecular reactions, at the heated substrate, produce individual crystallites which essentially aggregate and spread to produce a ceramic coating without associated carbonate problems. The P-E loops for NKN films made by alkoxide sol–gel processes exhibit significant dielectric losses, showing a

nonferroelectric resistor-capacitor (RC) component, even if excess alkali metal reagents are used to offset volatilization losses at film fabrication temperatures. The P-E response is not typical of a ferroelectric, as the loops show upward curvature on decreasing the applied field from its maximum value.³⁴ In sol–gel NKN processes, the persistence of carbonate second phases formed by interaction of the vapors of alkoxide decomposition products with the metal oxide species in the gels will contribute to residual dielectric losses. The resulting loops are, at best, a combination of a lossy dielectric response and a ferroelectric component.

Comparison with a Standard Sol–Gel PZT System

To aid a general comparison with a well-defined system exhibiting good ferroelectric properties and to investigate the differences observed in the thermal analysis plots, the TGA, DTA, and DTG plots for a dried $\text{PbZr}_{0.3}\text{Ti}_{0.7}\text{O}_3$ sol synthesized using a triol-based route were examined and these are shown in Figure 14. This plot may be compared to the thermal analysis plots of the dried NKN sol (Figures 1–5). The triol based route for PZT is a well established process that has been reported to produce very high-quality PZT films with excellent structural and electrical properties.^{35,36}

Here, as can be seen in Figure 14 from the DTA plot of a dried PZT sol–gel made from lead acetate and propoxides of zirconium and titanium (stabilized by acetyl acetone), the last exothermic heating peak is at ~480 °C. This is associated with a minor CO_2 evolution and is assigned to the formation of single-phase PZT. The exothermic peak at 323 °C signifies the onset of an organic

(33) Cho, C.-R. *Mater. Lett.* **2002**, *57*, 781.

(34) Ahn, C. W.; Lee, S. Y.; Lee, H. J.; Ullah, A.; Bae, J. S.; Jeong, E. D.; Choi, J. S.; Park, B. H.; Kim, I. W. *J. Phys. D: Appl. Phys.* **2009**, *42*, 215304.

(35) Naksata, M.; Brydson, R.; Milne, S. J. *J. Am. Ceram. Soc.* **2003**, *86*, 1560.

(36) Sriprang, N.; Kaewchinda, D.; Kennedy, J. D.; Milne, S. J. *J. Am. Ceram. Soc.* **2000**, *83*, 1914.

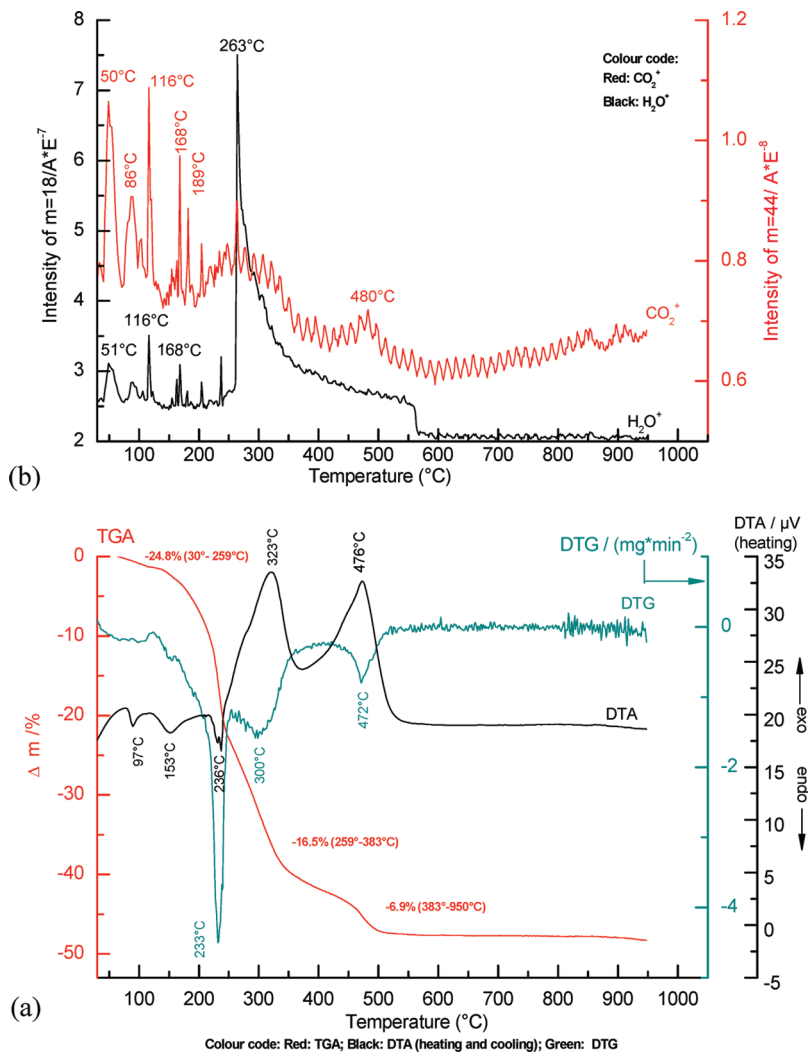


Figure 14. (a) TGA, DTG, DTA, and (b) mass spectrometry plots for the dried $\text{PbZr}_{0.3}\text{Ti}_{0.7}\text{O}_3$ sol synthesized using a triol-based route.

decomposition process. The endothermic peaks at the lower temperatures of 97 and 153 °C signify the loss of water (structural and physically adsorbed) and the final endothermic peak at 236 °C indicates the removal of further high-boiling-point organics. The TGA plot confirms the final decomposition step coincides with the crystallization temperature. The important point to note here, in contrast to the NKN system, is the presence of a single peak for the crystallization event and the absence of any subsequent thermal decomposition. The lead carbonates formed in the PZT system are much less stable than equivalent alkali metal carbonates in the NKN system. The carbonate decomposition in PZT films takes place at < 500 °C,³⁷ well below the decomposition temperatures of corresponding alkali metal carbonates. In addition, the DTA data indicate a single crystallization event in PZT, immediately following the carbonate decomposition. Hence, PZT single-phase ferroelectric films, free from residual carbonate phases, may be produced by heating at 600–700 °C.^{35,36} In the future, it would be useful to investigate the possibility of developing alter-

native Na, K, and Nb precursors, including long chain carboxylates which are less liable to decompose to release CO_2 and generate intermediate carbonates; such compounds have been developed for other ferroelectric ceramics.^{38–41}

Conclusions

The critical issues in the sol–gel processing of NKN thin films were identified through a detailed study of the thermochemistry of a metal alkoxide sol–gel system. The sols were prepared by dissolving Na and K metals in methoxyethanol followed by reaction with Nb ethoxide. Combined DTA–TGA–MS experiments showed the presence of two DTA crystallization peaks in the temperature range 480–550 °C, which are attributed to intermediate NKN phases, differing slightly in composition from the desired $\text{Na}_{0.5}\text{K}_{0.5}\text{NbO}_3$ phase. Extended reflux times (70 h) failed to produce a homogeneous sample displaying a

(37) Chowdhury, A.; Thompson, P. R.; Milne, S. J. *Thermochim. Acta* **2008**, *475*, 59.

(38) Ali, N. J.; Milne, S. J. *J. Am. Ceram. Soc.* **1993**, *76*, 2321.

(39) Ali, N. J.; Milne, S. J. *J. Mater. Res.* **2006**, *21*, 1390.

(40) Hasenkox, U.; Hoffmann, S.; Waser, R. *J. Sol-Gel Sci. Technol.* **1998**, *12*, 67.

(41) Hoffmann, S.; Waser, R. *J. Eur. Ceram. Soc.* **1999**, *19*, 1339.

single crystallization peak, although there was evidence that the compositional separation was reduced.

A heating DTA endothermic peak around 825–850 °C and sharp cooling exotherm at ~830 °C were consistent with melting and crystallization from the melt on cooling of sodium carbonate or a mixture of sodium and potassium carbonate secondary phases. This is a further example of chemical segregation within the gels and also indicates the thermal stability of the alkali metal carbonates. Additional mixed Na/K carbonate or bicarbonate phases were also formed in the sample (after high-temperature decomposition) as a result of exposure to the atmosphere.

The multiphase nature of ceramic films made using these sols, and particularly the occurrence of stable

carbonate phases, accounts for the failure to observe polarization-electric field hysteresis loops which do not have strong contributions from dielectric losses. This presents a fundamental impediment to the production of high-grade ferroelectric NKN thin films, particularly on platinized silicon substrates by the sol–gel method.

Acknowledgment. Anirban Chowdhury is grateful to the ORS Award Scheme (combined with Tetley-Lupton scholarships), SPEME, and IMR for providing financial assistance. Jonathan Bould acknowledges the support of the Academy of Sciences of the Czech Republic Grant No. M200320904. We thank Prof. J. D. Kennedy at the School of Chemistry, University of Leeds, for his kind support and cooperation. We are also very grateful to Dr. Billy Richards for his help in the experiments in thin film spectroscopy.